Appl Phys B (2012) 109:453–460
DOI 10.1007/s00340-012-5115-5

Applied Physics B
Lasers and Optics

Multimode diode laser correlation spectroscopy using gas-filled porous materials for pathlength enhancement

X.T. Lou · C.T. Xu · S. Svanberg · G. Somesfalean

Received: 5 July 2011 / Revised version: 5 June 2012 / Published online: 6 September 2012

Abstract A novel pathlength enhancement approach has been applied in multimode diode laser correlation spectroscopy measurements of gas concentrations. Reference and sample gas cells made of porous polystyrene foam and alumina ceramic, respectively, were employed in proof-of-principle measurements of molecular oxygen. Equivalent pathlengths of 164 and 52 cm were obtained for the reference and sample cells with physical pathlengths of 4 and 1 cm, respectively. With a measurement time of 60 s, a physical-pathlength-integrated sensitivity of 15 ppm·m was achieved with an enhancement of more than one order of magnitude compared with an open-air setup. Practical application aspects were investigated including gas cell size and light alignment tolerance. This generic approach for pathlength enhancement provides advantages in terms of compactness and robustness.

1 Introduction

Tunable diode laser absorption spectroscopy, TDLAS, has become a well-known diagnostic technique for gas detection due to its high sensitivity, speed and selectivity. To fulfill different requirements in specific applications, various alternative techniques based on TDLAS have been developed. One of them is a technique termed multimode diode laser correlation spectroscopy, MDL-COSPEC, which combines TDLAS with gas correlation spectroscopy [1]. MDL-COSPEC has been successfully demonstrated both for single and multiple gas detections [2, 3], presenting advantages of low-cost due to the utilization of cheap multimode diode lasers and high stability because of the employment of the correlation scheme. On the other hand, the sensitivity achieved by MDL-COSPEC is degraded by a typical factor of 5–10 since the integrated absorption magnitude is generally diluted by the non-absorbed laser modes.

A straight-forward method to improve sensitivity in diode laser absorption spectroscopy for point monitoring is by employment of multipass gas cells to increase the optical pathlength. Until now, three typical embodiments have been developed:

(a) White and Herriot cells [4, 5]. The laser beam is reflected between two carefully designed mirror surfaces to yield a multiple of the physical length of the cell. The pathlength enhancement is typically 100–500, e.g., 240 m pathlength was achieved by using a 47-cm Herriot cell [6].
(b) Cavity enhanced techniques [7–9]. In both cavity ring-down spectroscopy and cavity enhanced absorption spectroscopy (or integrated cavity output spectroscopy), a high-finesse optical cavity constructed by two highly reflecting concave mirrors is used to achieve a large pathlength enhancement. The pathlength enhancement can be $>10^3$ by using mirrors with reflectivities of >99.9 %, e.g., 19.2 km pathlength was achieved within a 115-cm optical cavity [10].
(c) Use of integrating spheres as gas cells [11]. Light is diffusively reflected within a relatively small volume to increase the pathlength. The pathlength enhancement is typically 10–50 with an internal surface reflectivity of 95 %–99 %, e.g., 114 cm pathlength was achieved with a spherical diameter of 5.1 cm [12].

X.T. Lou
Department of Physics, Harbin Institute of Technology, Harbin 150001, China

X.T. Lou · C.T. Xu · S. Svanberg · G. Somesfalean (✉)
Department of Physics, Lund University, 22100 Lund, Sweden
e-mail: gabriels@fysik.lth.se

Each of these multipass cell designs presents advantages in specific measurement applications. Method (a) is relatively straight-forward and provides a moderate pathlength enhancement with moderate complexity of alignment. Method (b) can provide, at present, the longest equivalent pathlength but suffers from time-consuming alignment and strict vibration tolerances. Compared with method (a) and (b), method (c) can only achieve an equivalent pathlength of a few meters, but it evidently offers advantages of relaxed alignment tolerances as well as compact volume.

An alternative approach can be based on the gas in scattering media absorption spectroscopy, GASMAS [13, 14], by using gas-filled porous materials as multipass cells. GASMAS has been applied in various fields including wood drying studies [15], food monitoring [16] and medical diagnostics [17], etc. In GASMAS, the equivalent pathlength in porous materials can easily be increased by one order of magnitude or more as compared with the physical length, which enables promising applications of scattering materials for pathlength enhancement [13, 18, 19]. In the present work, this new approach was applied to MDL-COSPEC. Compact and robust multipass cells made of polystyrene foam and alumina (Al_2O_3) ceramic with open pores were employed in a proof-of-principle setup for oxygen detection. The wavelength modulation spectroscopy (WMS) technique with second harmonic detection was employed to improve the signal-to-noise-ratio. Several aspects were addressed related to practical applications of scattering materials as gas sampling containers, including gas cell size, incident angle of laser beam, and the lateral as well as vertical displacement of the laser injection point relative to the detector.

2 Principles

2.1 Multimode diode laser correlation spectroscopy

The fundamental principle of MDL-COSPEC has been described previously [1–3] and will only be outlined here. Briefly, MDL-COSPEC is a combination of the TDLAS and gas correlation spectroscopy technique in which multimode diode lasers are employed. The multimode laser source can be regarded as a set of single-mode lasers with intensity distributions being randomly variable. By scanning the center wavelength of the multimode diode laser, absorption signals can be generated when one or more individual modes come into resonance with absorption lines of a gas. Using a reference cell with a well-calibrated concentration and pathlength of the target gas, the absorption signals from the sample gas can be isolated, enabling retrieval of the unknown concentration. The identification of target signals is based on the fact that the sample and the reference signals originating from the same species of gas are well correlated both in line shape and in magnitude ratio. Since the wavelength of diode lasers is sensitive to temperature, the operating temperature of the multimode diode laser is often varied (typically 3–10 K) in order to achieve a wide wavelength covering range, guaranteeing a nearly uniform distribution of the absorption probability over a long period of time.

2.2 Absorption spectroscopy in scattering materials

Translucent porous materials are light scattering materials which have tiny internal structures capable of holding gases. Light injected into these materials will be heavily scattered, propagating through the material via different paths and yielding different pathlengths. The diffusively transmitted light has thus typically traveled a much larger distance as compared with the physical dimension of the porous scattering material. As mentioned above, detection of gases within translucent scattering materials can be enabled with the GASMAS technique [13, 14]. The technique is based on the fact that the absorption imprints from solids as compared with gases are fundamentally different, i.e. the absorption profile of a solid is much broader than that of a gas. By tuning the wavelength of the source to specific gas absorption lines while scanning the frequency, it is thus possible to extract the gas absorption imprint from the broad and slowly varying absorption of a solid, even though the absorption of a solid is typically orders of magnitude larger than that of a molecular gas. However, the lack of direct information about the optical pathlength prevents the straight-forward utilization of the Beer–Lambert Law. Therefore, the concept of equivalent pathlength was introduced and defined as the mean distance that light passes through gases dispersed in the scattering medium.

3 Experimental details

3.1 Gas cells made of porous materials

In the present work, a polystyrene foam slab with a 39 mm thickness and 98 % porosity [18] was employed as the reference gas cell, and an alumina ceramic plate with a 10 mm thickness and 34 % porosity [19] was employed as the sample gas cell. The ambient atmosphere filled the porous gas cells for demonstration measurements on molecular oxygen. Table 1 summarizes the main properties of these two types of material with different advantages and disadvantages due to their characteristic differences in material properties.

Since polystyrene foams have a better capability of light transmission than alumina ceramics, a 13 mm^2 photodiode (DET 110, Thorlabs) was used for the former while an

Table 1 Summary of the main properties of the employed polystyrene foam and alumina ceramic. Thickness (d), porosity (p), transport scattering coefficient (μ), detected light fraction (f), equivalent pathlength (L_{eq}), pathlength enhancement (E), gas exchange time (t)

Material	d (mm)	p (%)	μ (cm^{-1})	f (%)	L_{eq} (cm)	$E = L/d$	t
Polystyrene foam [18]	39	98	40	0.01	164±2	~42	~2 h
Al_2O_3 ceramic [19, 20]	10	34	1300	0.02	52±1	~52	<10 s

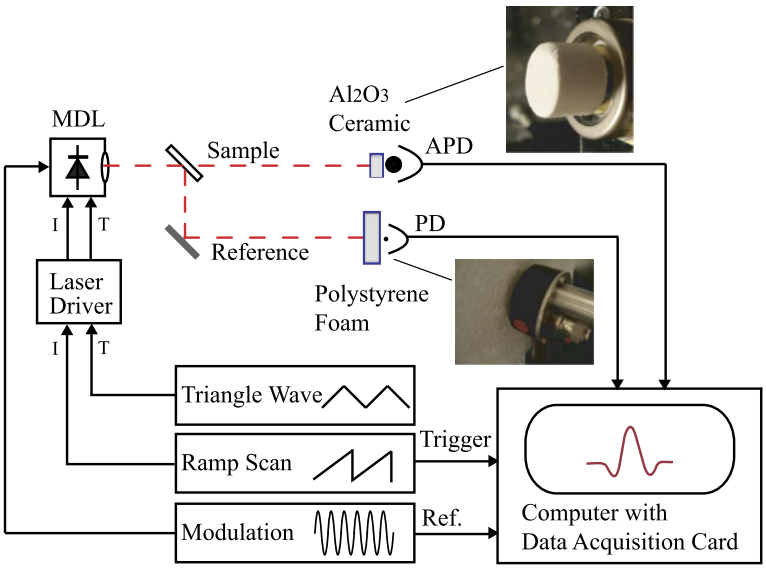

Fig. 1 Schematic of the experimental setup for MDL-COSPEC using polystyrene foam and alumina ceramic as reference and sample gas cells, respectively

avalanche photodiode (SD394-70-72-661, Advanced Photonix) with a larger area of 79 mm^2 was used for the latter. Despite being thicker and suffering from a smaller detector area, the polystyrene foam sample achieves a comparable amount of light for detection as the alumina ceramic plate, as indicated in Table 1. The detected light power was around 1 μW. For materials with strong scattering properties, the equivalent pathlength is proportional to the square of the thickness, i.e. $L_{eq} \sim d^2$ [18]. The equivalent pathlengths of the polystyrene foam slab and the alumina ceramic plate were measured to be 164 ± 2 cm and 52 ± 1 cm, respectively. The equivalent pathlength was determined by the ratio between the oxygen absorption signals from these air-filled porous materials and that of the ambient air with a known pathlength. The gas exchange time, however, for the polystyrene foam is about three orders of magnitude longer than that of the alumina ceramic [18, 20]. Hence, the alumina ceramic plate is more applicable as a sample gas cell due to the fast gas invasion speed; whereas the polystyrene foam slab is more applicable as a reference cell since it can provide a longer equivalent pathlength yielding better signal-to-noise-ratio, which is particularly important for the MDL-COSPEC technique.

3.2 Configuration

The setup of the MDL-COSPEC is mainly based on the TDLAS instrumentation in combination with a correlation scheme, as schematically shown in Fig. 1. The oxygen concentration in ambient air was assumed to be a constant of 20.9 vol.%. Figure 2(a) shows the HITRAN-calculated A-band absorption of ambient oxygen around 760 nm [21].

The Fabry–Pérot type multimode diode laser (LT031-MDO, Sharp) had a center wavelength distribution around 755 nm at 25 °C with a maximum output power of 7 mW. In order to overlap the emission spectrum of the laser with the absorption lines of oxygen, its operating temperature was raised. The recorded multimode emission spectrum of the diode laser operating at 45 °C and 67 mA is shown in Fig. 2(b). To perform WMS, the laser wavelength was scanned by a 24-Hz injection current ramp from 60 to 73 mA through a current driver (LDC 201C, Thorlabs), and a sinusoidal signal of 20 kHz was directly coupled into the laser. In order to achieve a wide wavelength covering range, the working temperature of the diode laser was varied from 44 to 47 °C through a temperature controller (TED 200C, Thorlabs) by adding a triangle voltage signal at 0.1 Hz.

The laser output was split into two beams passing through the sample and the reference gas, respectively. The signals in the two detection arms were simultaneously acquired using a 14-bit DAQ card (PCI-6132, National Instrument) and demodulated at 40 kHz by a LabVIEW-based lock-in software to obtain the WMS-2f signals.

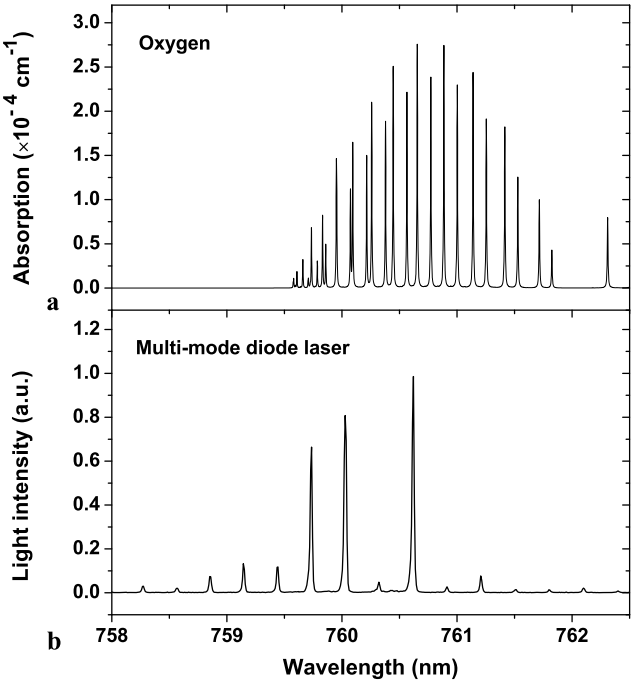

Fig. 2 (**a**) Absorption spectrum for 20.9 vol.% oxygen around 760 nm; (**b**) emission spectrum of the employed multimode diode laser

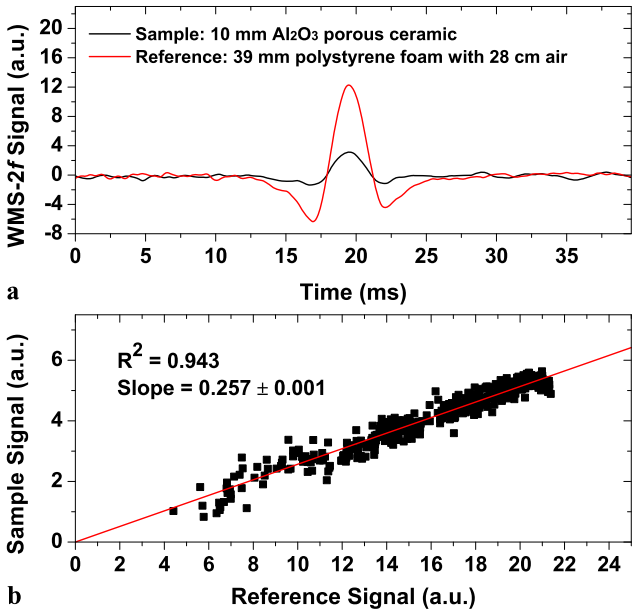

Fig. 3 (**a**) Typical WMS-2f signal pairs of oxygen in a 42-ms ramp scan; (**b**) signal pair magnitudes acquired during 20 s due to random multimode absorptions

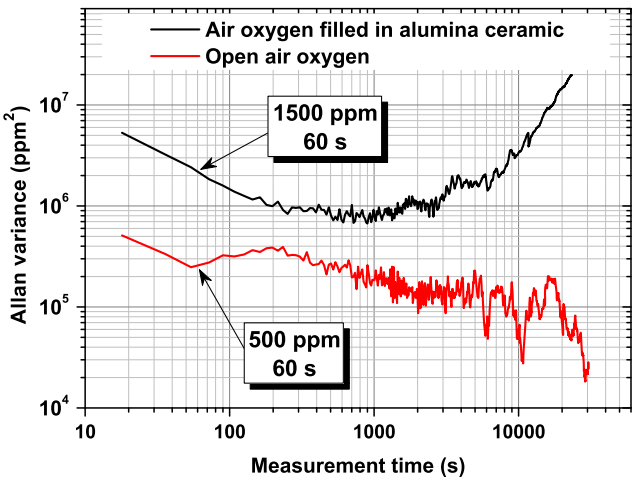

Fig. 4 Allan variance plots for successively measured concentrations of air oxygen filled in 10 mm alumina ceramic over a 13-hour period and of oxygen in 32 cm open air over a 17-hour period

4 Measurement and results

A typical WMS-2f signal pair within a 42-ms ramp scan is shown in Fig. 3(a). The sample signal shows the total absorption signal subtracted by the absorption signal offset, originating from 39-cm pathlength in ambient oxygen. The reference signal includes absorption signals of oxygen both in the polystyrene foam slab and in a 28-cm pathlength of ambient air. Figure 3(b) shows an accumulation of recorded signal pair magnitudes acquired during 20 s. The slope of linear-regression gives the absorption signal ratio representing the equivalent-pathlength-integrated concentration.

The performance of the proposed MDL-COSPEC system in terms of sensitivity and stability was evaluated using Allan variance analysis [22] on 13-hour successive measurements. For comparison, Allan variance analysis was also performed on 17-hour continuous measurements using 32-cm of open path in ambient air as the sample gas and a photodiode as the detector. Allan variance plots for both two cases are shown in Fig. 4, indicating that with a measurement time of 60 s, sensitivities of 1500 and 500 ppm, respectively, can be achieved. The corresponding physical-pathlength-integrated sensitivities—i.e., physical pathlength times sensitivity—are 15 and 160 ppm·m, respectively. It indicates that the sensitivity was improved by a factor of 11 by using such a sample gas cell of alumina ceramic. It is worth noting that the sensitivity reported here is integrated by the physical pathlength instead of the commonly used effective pathlength in order to emphasize the merit of compactness of the gas sample cells made of porous materials. Although compact gas sensors can also be designed utilizing miniature multipass cells, porous-material-based gas cells can achieve better compactness (with volumes < 1 cm^3) and—as proved in Sect. 5—provide superior tolerances for laser beam alignment.

The sensitivity improvement achieved, however, is only about $1/5$ compared with the pathlength enhancement (52), which is mainly due to the interference noise. In conventional gas-sensing systems based on coherent sources, most interference fringes are caused by Fresnel reflections be-

tween smooth optics such as gas cell windows, lenses and mirrors, etc. In contrast, the main interference noise for the present system is caused by the highly diffuse surface and porous scattering structure of the ceramic material, corresponding to feedback interference (due to the light reflected back into the laser diode) and speckle interference (due to the light scattered by a randomly scattering structure), respectively [23]. Comparisons of these two categories of interference noise have been reported in [24], concluding that it is speckle interference noise that limits the final sensitivity. For more dense samples (with high absorption coefficients or large thicknesses) shot noise could be the limiting factor. The interference noise also degraded the long-term stability, as is shown in Fig. 4. Over a 13 hour period, the system using the alumina ceramic gas cell drifted about three times the sensitivity, while without utilization of the alumina ceramic gas cell the measurement drift was less than the sensitivity.

5 Consideration for practical applications

In practical applications of porous materials utilized as gas sampling containers, several aspects have to be considered in terms of gas cell size and light alignment tolerance. For a porous cell with a certain thickness, the diameter of the cell should be designed as small as possible to achieve a fast gas exchange time, while it should also be large enough to neglect edge effects, i.e. the gas cell can be considered to be laterally infinite and thus appears homogeneous for the diffusively transmitted light. Light alignment issues mainly address the incident angle of the laser beam, and the lateral as well as vertical displacement of the laser injection point from the detector.

5.1 Edge effects

The edge effects of three slabs of polystyrene foam with thicknesses of 29, 39 and 49 mm, respectively, were measured by moving the polystyrene foam samples, keeping the positions of the laser injection spot and the detector fixed. Figure 5(a) plots the equivalent pathlength versus the lateral distance of the measurement spot from the edge of the polystyrene foam. A schematic setup is also shown in the insets. Because of the increased loss of light exiting the material, the equivalent pathlength starts to decrease significantly (less than 95 % of the original value corresponding to an infinite sample) when the distance between the measurement spot and the edge of the polystyrene foam is smaller than about 0.7 times the thickness of the scattering sample. Thus the ratio between the diameter and the thickness of the polystyrene foam gas cell should be at least ∼1.4 in order to eliminate edge effects. For the sake of completeness, the edge effect of the alumina ceramic listed in

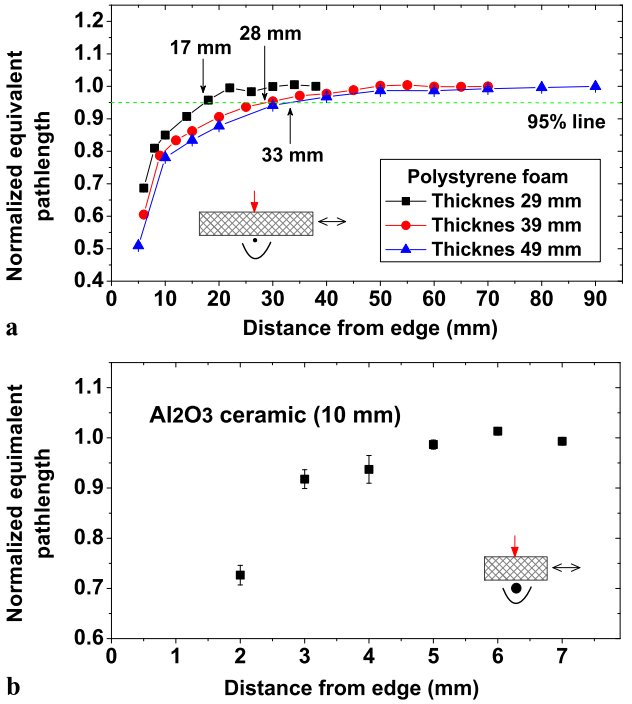

Fig. 5 Dependence of the equivalent pathlength on the distance between measurement spot and the edge for: (**a**) polystyrene foams with different thicknesses of 29, 39, and 49 mm, respectively; (**b**) 10-mm thick alumina ceramic

Table 1 with a diameter of 14 mm was measured and is shown in Fig. 5(b). When the measurement spot is 0.5 times the thickness from the edge, the edge effect is negligible, which is generally consistent with the measurement results of polystyrene foam. The discrepancy originates from the difference of relative detection area to the sample size, as for the alumina ceramic an APD with a relatively larger area was used, leading to a decreased sensitivity to edge effects.

5.2 Incident angle

The incident-angle effect was measured by changing the incidence angle of the laser while having the positions of the incident spot and the detector fixed. Figure 6 shows the measurement results for polystyrene foam and alumina ceramic. We believe that the obtained measurement error is mainly caused by interference fringes. Compared with polystyrene foam, alumina ceramic yields larger optical interference due to higher surface reflectivity, thereby leading to a larger noise level. However, within the measurement error, the variances of the equivalent pathlength of both polystyrene foam and alumina ceramic are less than 5 % even after changing the laser incident angle by more than 40 degrees. It indicates a great tolerance of the laser incident angle for practical applications.

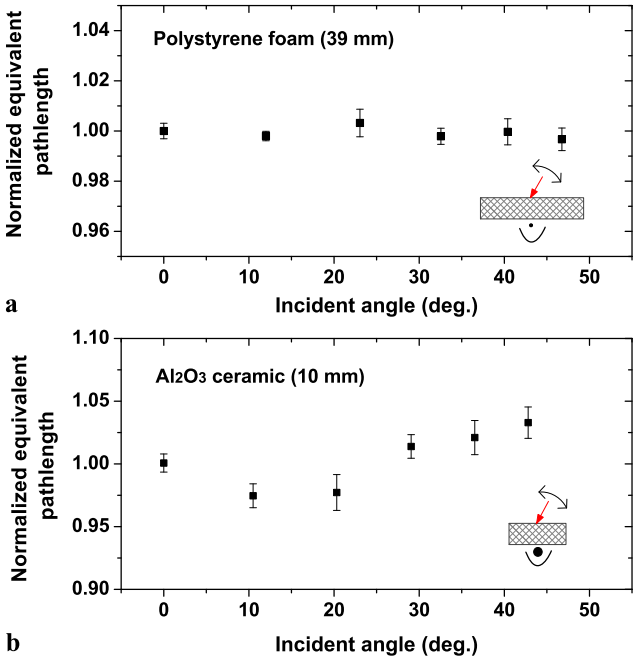

Fig. 6 Dependence of the equivalent pathlength on the incident angle of the laser beam for: (**a**) polystyrene foam; (**b**) alumina ceramic

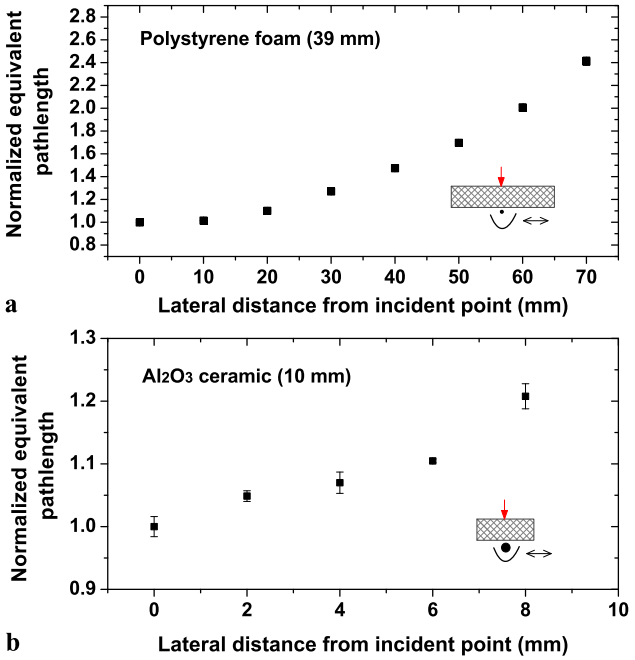

Fig. 7 Dependence of the equivalent pathlength on the lateral distance of the detector from the incident laser point for: (**a**) polystyrene foam; (**b**) alumina ceramic

5.3 Detection lateral deviation

The effect of lateral deviation was measured by moving the detector laterally relative to the injection point. In fact, this would be equivalent to move the laser injection position a same relative distance to the detector. Figure 7 shows the measurement results for polystyrene foam and alumina ceramic. The equivalent pathlength becomes longer as the lateral distance of the detector from the laser injection point increases, which is in good agreement with the results in Ref. [18]. Figure 7(a) clearly shows that the profile is relatively flat near the zero position, indicating that a small lateral displacement of the laser injection spot or the detector position does not significantly affect the achieved pathlength. This property is of great relevance as it is then possible to construct compact and robust systems with considerable tolerances. For example, within a lateral displacement 0.2 times the thickness of the scattering material, the relative discrepancy of equivalent pathlength is less than 5 %.

5.4 Detection vertical deviation

The effect of vertical deviation was measured by vertically moving the detector relative to the sample surface. Figure 8 shows the measurement results for polystyrene foam and alumina ceramic. The figure shows that the equivalent pathlength with respect to the vertical distance of the detector depends on the area of the detector relative to the sample area. In the case of polystyrene foam, the photodiode only covers a small central part of the sample. Therefore, as it moves away from the sample surface, it will receive more and more photons emerging with larger lateral displacements, leading to an increase in the equivalent pathlength. The reverse is also true. For the alumina ceramic, when the APD—which

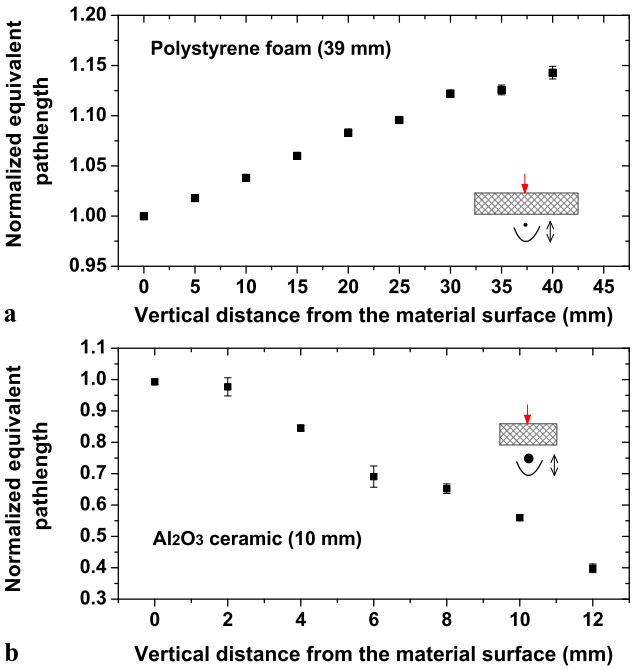

Fig. 8 Dependence of the equivalent pathlength on the vertical distance of the detector from the scattering material surface of the (**a**) polystyrene foam; (**b**) alumina ceramic

covers more than half the area of the sample—moves away, the equivalent pathlength will decrease due to the decreased collection of light from large lateral displacement positions.

6 Discussion and conclusions

As mentioned above, the achieved pathlength enhancement using scattering materials can further be improved by increasing the sample thickness and/or the lateral distance between the laser injection point and the detector. However, these two measures are all at the cost of reducing the fraction of the detected light due to the increased scattering attenuation. The dependence of the detected laser power on the thickness was also theoretically predicted and measured in Ref. [18]. Under shot noise limited conditions, the reduction of the received light intensity would certainly degrade the sensitivity [25]. Therefore there is a trade-off between the increase of the equivalent pathlength and the reduction of the detected light. The optimal arrangements to obtain the best signal-to-noise-ratio depend on the material and the laser power. Materials possessing both favorable absorption and scattering properties are ideal for achieving a good sensitivity. Compared with the absorption signal, the interference noise is independent on the laser power; thus the sensitivity can definitely be improved by employment of a high-power laser in combination with a thick scattering material, which is relatively straight-forward to implement. In general, multimode diode lasers have much higher output power and better availability than single-mode varieties, which can greatly compensate for the sensitivity degradation due to diluted absorption magnitude by residual laser modes.

Another important material-related issue is the gas exchange time. In practical applications, the gas exchange constant should at least be less than the data processing time, including signal averaging; otherwise it would become the bottleneck for the response time for the whole gas-sensing system. For MDL-COSPEC, since the reference gas cell does not need gas exchange, gas exchange times in the order of hours are required for manufacture. For example, although polystyrene foam presents a superior combination of high absorption and scattering properties, it is not suitable to be used as a sample gas cell. However, it can still be fully utilized as a reference gas cell because of its acceptable gas exchange time (in the order of hours [18]).

Considering their suitability for practical applications, several aspects including edge effects and light alignment issues were experimentally investigated, showing that gas cells made of porous scattering materials present exceptionally relaxed alignment tolerance and thus can be readily employed. Edge effects can be effectively eliminated by using pieces with diameters larger than 1.4 times the sample thickness. The measurement is insensitive to the laser incident angle. Small displacement of the laser injection spot from the detector position does not significantly affect the measurement results.

Generally, compared with conventional pathlength enhancement methods, the advantages of porous-material-based gas cells are their great compactness and high alignment tolerance. For example in the case of the cavity enhanced techniques, the cavity length should be in the order of tens of centimeters in order to achieve an acceptable spectral resolution, and strict optical alignment is required. Traditional multipass cells and integrating-sphere-based gas cells can be made with physical pathlengths of a few centimeters, but it is difficult to achieve a total volume of the gas cell less than 1 cm^3, which, however, can easily be realized by using porous-material-based gas cells. Furthermore, porous-material-based gas cells does not require good beam quality and possess more relaxed light alignment tolerance than multipass cells and can achieve larger pathlength enhancement than integrating-sphere-based gas cells. This kind of compact and alignment-free gas cells is particularly suitable in applications where gases in small cavities are to be detected.

To conclude, we have demonstrated optical-pathlength enhancement for MDL-COSPEC systems by using porous scattering materials as multipass cells. Proof-of-principle measurements of oxygen were performed. A 39-mm thick polystyrene foam slab and a 10-mm thick alumina ceramic plate were employed as reference and sample gas cells, with corresponding equivalent pathlengths of 164 ± 2 and 52 ± 1 cm, respectively. Allan variance analysis shows that with a measurement time of 60 s, a sensitivity of 1500 ppm can be achieved. The corresponding physical-pathlength-integrated sensitivity, 15 ppm·m, has been improved more than one order of magnitude compared with an open-air setup. This approach for pathlength enhancement, which is advantageous for constructing a compact and robust gas-sensing system, is particularly helpful in applications for multi-species detection by using MDL-COSPEC, where employment of several reference gas cells is required.

Acknowledgements This work was supported by a direct Swedish Research Council grant (621-2011-4265), the Natural Science Foundation of China (NSFC) (grant 61008027), the Fundamental Research Funds for the Central Universities (grant HIT.NSRIF.2009063) and a Linnaeus grant to the Lund Laser Centre. X.T. Lou and G. Somesfalean are grateful for Erasmus Mundus External Cooperation Window scholarships from the European Commission.

References

1. G. Somesfalean, M. Sjoholm, L. Persson, H. Gao, T. Svensson, S. Svanberg, Appl. Phys. Lett. **86**, 184102 (2005)
2. X.T. Lou, G. Somesfalean, B. Chen, Y.G. Zhang, H.S. Wang, Z.G. Zhang, S.H. Wu, Y.K. Qin, Opt. Lett. **35**, 1749 (2010)

3. X.T. Lou, G. Somesfalean, B. Chen, Z.G. Zhang, Appl. Opt. **48**, 990 (2009)
4. J.U. White, J. Opt. Soc. Am. **32**, 285 (1942)
5. D. Herriott, H. Kogelnik, R. Kompfner, Appl. Opt. **3**, 523 (1964)
6. J.B. McManus, M.S. Zahniser, D.D. Nelson, Appl. Opt. **50**, A74 (2011)
7. A. O'Keefe, D.A.G. Deacon, Rev. Sci. Instrum. **59**, 2544 (1988)
8. R. Engeln, G. Berden, R. Peeters, G. Meijer, Rev. Sci. Instrum. **69**, 3763 (1998)
9. A. O'Keefe, Chem. Phys. Lett. **293**, 331 (1998)
10. J.M. Langridge, T. Laurila, R.S. Watt, R.L. Jones, C.F. Kaminski, J. Hult, Opt. Express **16**, 10178 (2008)
11. D. Masiyano, J. Hodgkinson, R.P. Tatam, Appl. Phys. B **100**, 303 (2010)
12. E. Hawe, P. Chambers, C. Fitzpatrick, E. Lewis, Meas. Sci. Technol. **18**, 3187 (2007)
13. M. Sjöholm, G. Somesfalean, J. Alnis, S. Andersson-Engels, S. Svanberg, Opt. Lett. **26**, 16 (2001)
14. S. Svanberg, Laser Phys. **20**, 68 (2010)
15. M. Andersson, L. Persson, M. Sjöholm, S. Svanberg, Opt. Express **14**, 3641 (2006)
16. M. Lewander, Z.G. Guan, L. Persson, A. Olsson, S. Svanberg, Appl. Phys. B **93**, 619 (2008)
17. L. Persson, M. Andersson, M. Cassel-Engquist, K. Svanberg, S. Svanberg, J. Biomed. Opt. **12**, 054001 (2007)
18. G. Somesfalean, M. Sjoholm, J. Alnis, C. af Klinteberg, S. Andersson-Engels, S. Svanberg, Appl. Opt. **41**, 3538 (2002)
19. T. Svensson, E. Adolfsson, M. Lewander, C.T. Xu, S. Svanberg, Phys. Rev. Lett. **107**, 143901 (2011)
20. T. Svensson, M. Lewander, S. Svanberg, Opt. Express **18**, 16460 (2010)
21. L.S. Rothman, I.E. Gordon, A. Barbe, D.C. Benner, P.E. Bernath, M. Birk, V. Boudon, L.R. Brown, A. Campargue, J.P. Champion, K. Chance, L.H. Coudert, V. Dana, V.M. Devi, S. Fally, J.M. Flaud, R.R. Gamache, A. Goldman, D. Jacquemart, I. Kleiner, N. Lacome, W.J. Lafferty, J.Y. Mandin, S.T. Massie, S.N. Mikhailenko, C.E. Miller, N. Moazzen-Ahmadi, O.V. Naumenko, A.V. Nikitin, J. Orphal, V.I. Perevalov, A. Perrin, A. Predoi-Cross, C.P. Rinsland, M. Rotger, M. Simeckova, M.A.H. Smith, K. Sung, S.A. Tashkun, J. Tennyson, R.A. Toth, A.C. Vandaele, J. Vander Auwera, J. Quant. Spectrosc. Radiat. Transf. **110**, 533 (2009)
22. P. Werle, Appl. Phys. B **102**, 313 (2011)
23. J. Hodgkinson, D. Masiyano, R.P. Tatam, Appl. Phys. B **100**, 291 (2010)
24. T. Svensson, M. Andersson, L. Rippe, J. Johansson, S. Folestad, S. Andersson-Engels, Opt. Lett. **33**, 80 (2008)
25. P. Werle, Spectrochim. Acta A **54**, 197 (1998)